MÜHENDİSLİK ve DOĞA BİLİMLERİ FAKÜLTESİ

Uluslararası Mühendislik Araştırma ve Geliştirme Dergisi
International Journal of Engineering Research and Development

UMAGD, (2024) 16(2), 550-563.

10.29137/umagd.1390384

Cilt/Volume:16 Sayı/Issue:02 Haziran/June 2024

Araştırma Makalesi / Research Article

Investigation of Hydraulic Effect in Terms of Colloid Formation From Compacted Bentonite

Sıkıştırılmış Bentonitten Kolloid Oluşumu Açısından Hidrolik Etkinin İncelenmesi

Süleyman Bülbül[1*]

[1]*Karamanoğlu Mehmetbey Üniversitesi, Sosyal Bilimler Meslek Yüksek Okulu, 70100 Karaman, TÜRKİYE*

***Başvuru/Received**: 13/11/2023.* ***Kabul/Accepted**: 26/01/2024* ***Çevrimiçi Basım/Published Online:** 30/06/2024*
***Son Versiyon/Final Version**: 30/06/2024*

Abstract

A series of experiments were conducted an investigation into the amount of erosion, size of eroded particles, and swelling area of physically purified and compacted bentonite under different flow rates. Dynamic light scattering method(DLS) was used to determine the size and amount of eroded particles and Autocad programme was used to determine the swelling area.Where compacted bentonite and crushed granite come into contact, groundwater plays an important role in the erosion of bentonite.Contact of compacted bentonite with water, its saturation with water and its subsequent swelling and entry into the voids around it are the primary steps for the formation of colloid particles. Factors affecting the erosion of compacted bentonite are groundwater flow rate, ionic strength of the water contacting the bentonite, pH of the water, etc. The groundwater to which the compacted bentonite buffer will be exposed during the designed service life of the compacted bentonite buffer reduces the robustness of the bentonite buffer.Erosion of compacted bentonite not only affects its physical stability but also causes the transport of radionuclides it absorbs.An experimental methodology is presented. The experimental results showed that with increasing flow rate the amount of eroded bentonite increases and the swelling area increases. No correlation was found between the flow rate and the size of the eroded particles.

Key Words

"Bentonite, colloids, stability, waste repository"

Öz

Fiziksel olarak saflaştırılmış ve sıkıştırılmış bentonitin farklı akış hızları altında erozyon miktarı, aşınan parçacıkların boyutu ve şişme alanı üzerine bir dizi deney yapılmıştır. Aşınan parçacıkların boyutunu ve miktarını belirlemek için dinamik ışık saçılımı yöntemi (DLS) ve şişme alanını belirlemek için Autocad programı kullanılmıştır. Sıkıştırılmış bentonit ve kırılmış granitin temas ettiği yerlerde, yeraltı suyu bentonitin aşınmasında önemli bir rol oynar. Sıkıştırılmış bentonitin su ile teması, su ile doygunluğu ve ardından şişmesi ve etrafındaki boşluklara girmesi, kolloid parçacıkların oluşumu için birincil adımlardır. Sıkıştırılmış bentonitin aşınmasını etkileyen faktörler yeraltı suyu akış hızı, bentonitle temas eden suyun iyonik gücü, suyun pH'ı vb.dir. Sıkıştırılmış bentonit tamponun tasarlanan hizmet ömrü boyunca maruz kalacağı yeraltı suyu bentonit tamponun sağlamlığını azaltır Sıkıştırılmış bentonitin erozyonu sadece fiziksel stabilitesini etkilemekle kalmaz, aynı zamanda emdiği radyonüklitlerin taşınmasına da neden olur Deneysel bir metodoloji sunulmuştur. Deneysel sonuçlar, artan akış hızı ile aşınan bentonit miktarının arttığını ve şişme alanının arttığını göstermiştir. Akış hızı ile aşınan parçacıkların boyutu arasında bir korelasyon bulunamamıştır.

Anahtar Kelimeler

"Bentonit, kolloids, stabilite, atık depolama"

***Corresponding Author: suleymanbulbul@kmu.edu.tr**

1. Introduction

Keeping spent nuclear at a certain depth in the ground for safe storage is currently a preferred alternative. The horizontal and vertical storage of high-level radioactive wastes in rocks rich in clay, salt and crystals at a certain depth in the ground is considered to be an appropriate environment as it provides the necessary conditions for the safe storage of these wastes. (Chapman and McKinley, 1987). Once the spent nuclear fuel can is put, the void between the cans and neighbouring solid soil particles and stones are repleted with shild which makes an engineered barricade. Owing to its high watertight, punctureless assets, ability to soak up water, resilience in the nature, bentonit has been chosen as an appropriate material for getting rid of spent nuclear. (Smith, 1980; Cho et al., 1999). On account of its low liquid content resulting from its natural structure, the bentonite mass used in storage cavities a certain amount below the surface has an extensive expansion prospective. By soaking up water vapour from adjanent solid soils, the bentonite mass will become sodden. Nevertheless, the bentonite mass used underground storage will not be completely soaked up with liquid within the calculated plan. The entrance of groundwater with low ionic strength into the storage area is also likely throughout time of congelation, which can continue for millennia and can be repeatable to eight repeatedly in the course of the typical storage assessment duration of one million years (AB, S. K. 2011).

Saturated compacted bentonite has an extensive enlargement force and is not at the start in balance with the neighbouring liquids and solid soils. Enlargement of compacted bentonite can also cause bentonite to enter open void open rock cavities. (Baik et al.,2007). By centering on the prospective generation of bentonite tiny pieces at underground where liquid, solid soil and bentonite meet, the following possibilities are suitable. (Grindrod et al.,1999).

Should the solidness of a condensed bentonite buffer becomes very down owing to enlargement, the saturated bentonite tiny pieces will dissociate and the observable way of acting of the bentonite turns into bentonite gel. Single tiny pieces of compacted bentonite may turn into untied or is stripped from the surface by the tangential movement of groundwater or it simply disperses into free particles. The colloid regime can be seen in terms of particle size. The generation of tiny bentonite pieces in a region the place the condensed clay meet groundwater may be crucial to the change of address of radioactive isotopes. This is because these radioactive isotopes are incorporated by the bentonite particles. Cho et al. (1999) have conducted experimental studies on radioactive isotopes relocation in Grimsel test area. In their studies, they determined the relationship between bentonite colloids and radioactive isotopes. The translocating way of acting of the tri- and tetravalent actinide Americium (Am) and Plutonium (Pu) was in a powerful way facilitated by tiny bentonite pieces in their research findings. The regainig was enhanced from 20% to 30% in the non-attendance of tiny bentonite pieces and to around 60-80% in the attendance of tiny bentonite pieces. The indicated illlustrates that even a small quantity of concentration losing in the bentonite material is unacceptable. The unclear point here is what size bentonite particles carry the radionuclides while the radionuclides are transported by bentonite. Since this problem has not been answered so far, the consequence of different hydraulic on the size of eroded bentonite particles will be important in the future when the relationship between radionuclide sorption and the size of eroded bentonite particles is found. Therefore, the size of eroded bentonite particles is shown daily throughout the experiment.

Kurosawa et al. (1999) conducted investigational and conceptual works to elucidate the capacity of water touching clay to generate tiny clay pieces. They decided that the results of tiny clay pieces on radioactive isotopes relocation is probably trivial in conducting assessment of spent nuclear getting rid of in between 500 meters and 1000 meters underground. Nonetheless, it has been observed in the research that small bentonite particles can sometimes occur at the junction of bentonite and underground rocks (Missana et al.,2003; Gecheis et al.2004; Schäfer et al.2012). Min Hoon Baik et al. (2007) found that tiny clay pieces could be abraded and relocated at the intersection of the compressed clay and apertured rock by a flowing groundwater relying on the flow rate of the groundwater, the contact time, and the chemical of contacting water. The influence of flow rate on the erosion of compacted bentonite has been investigated by some researchers (Baik et al.,2007; Vilks et al.,2010; Schatz et al.,2013). These three researchers observed that the bentonite particles eroded increased with increasing flow rate. The proportions of smectite in the compacted bentonite they used, the experimental set-ups they used, the weights of the bentonite they used and the amounts of the fracture aperture where the water acts on the bentonite are different from each other.

The aim of this study is to investigate the amount of erosion, size of eroded particles and swelling area of compacted bentonite used in the storage of spent nuclear fuel in relation to the flow rate during expected water ingress.

2. Experimental

2.1. Untreated bentonite

Voclay bentonite used in this investigation was obtained from Amcol company in the United Kingdom in 2018. The material and compound assets of Voclay clay were illustrated in table 1.

Table 1. Material and compound assets of the bentonite utilized in this investigation.

Assets	Percentage
Clay friction (%)	56
Smectite content (%)	86.8
Accessory minerals (%)	13.2
Quartz	3.9
Plagioclase	5.6
K-feldspar	0.9
Pyrite	0.2
Gypsum	trace
Compositions (%)	SiO_2= 62.30, Al_2O_3 = 19.13, Fe_2O_3= 10.31, CaO = 3.70, K2O = 1.39, MgO =1.52, P2O5 = 0.38, TiO_2= 0.39
Water content (%)	11.8
Liquid limit (%)	435
Plastic limit (%)	51.9
Specific gravity	2.73
External surface area (m2/g)	19.98
Total surface area(m2/g)	527
CEC (meq/100g)	93,9
Exchangeable cations (meq/100g)	Na^+=55,9, Ca^{2+}=30,1, Mg^{2+}= 6,9, K^+=1.1

The cation exchange capacity (CEC) of the Voclay bentonite was 93,9 meq/100g and Na^+ was a primary interchangeable cation.

2.2. Bentonite with reduced accessory minerals

In order to measure the erosion of compacted bentonite at dissimilar hydraulic values, the content of clay material was homogenised by physically purifying it. Accessory minerals restrict the implementation of poor-quality bentonite, causing a great waste of assets. Gong et al., (2016) proposed a basic procedure consist of crushing, scattering and separation was adjusted to increase a montmoriilonite content of poor-quality bentonite from Zhejiang, China. In their investigation, the montmorillonite ingredient of the clay improved from 44% to 96.5%. The procedure of increasing the content of montmorillonite is as follows:

- 3 g of crushed bentonite was mixed with 36 g of ionised water by adding 0.06 g of sodium hexametaphosphate (NaPO3)6 as shown in figure 1.
- As shown in figure 1, mixed for one day. In figure 3, following one day of mixing and removing the part remaining on the top of the polypropylene tube, the majority of the minerals other than montmorillonite stayed at the lowest part of the tube.
- The supernatant of the mixture was isoleted by centrifugation at a fixed position for two minutes. The increased montmorillonite contented bentonite was acquired following a centrifugation at 4500 r/min for two minutes as shown in figure 2.
- Following obtaining upper part from polypropylene tube, the upper part of liquid gathered in the glass bottle and placed to oven to dehydrate. In Figure 4, the majority of the minerals other than montmorillonite stayed in the polypropylene tube following upper part of tube was taken.

Figure 1. Mixing of clay-water composition

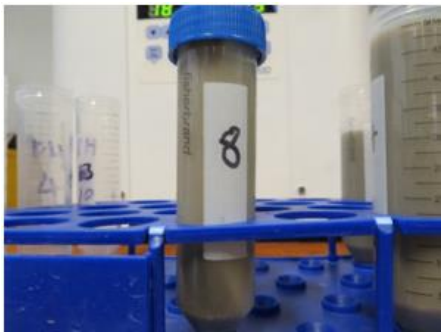

Figure 2. Clay-water sludge following centrifuge.

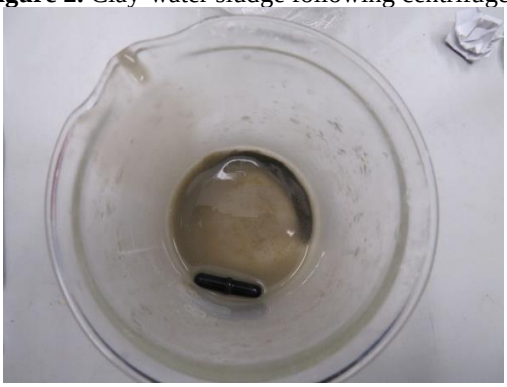

Figure 3. The slurry stayed at lowest part following one day of mixing.

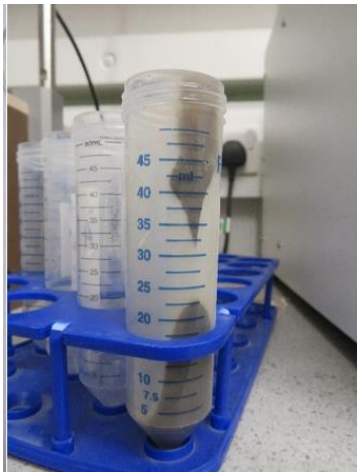

Figure 4. The tube following separation procedure.

Table 2. Differences between treated and untreated bentonite in terms of ingredient.

Ingredients	Untreated bentonite	Treated bentonite
Quartz	3.9	0.5
Plagioclase	5.6	trace
K-feldspar	0.9	0
Pyrite	0.2	0
Gypsum	trace	0
Opal-C	2.6	2.7
Smectite(Di)	86.8	96.8
Kaolinite	0	trace

Table 2 shows the percentage change in the content of treated and untreated bentonite.
The new water content obtained after the operations was found to be 8.11 per cent. Compressed bentonite samples in the form of a cylinder with a length of 1 cm and a radius of 1 cm were obtained.

2.3. Experimental setup and distilled water

Perspex, a glassy and sturdy substance, was selected to imitate prospective liquid entrance to the below the surface spent nuclear fuel storage. Owing to its glassy asset, it enabled us the chance to obtain images for the investigations. Therefore, expansion of compressed bentonite was examined during the experiments. 3 mm aperture test fixture was utilized. In figure 5, the width and length of 3-mm fracture experimental apparatus are illustrated.

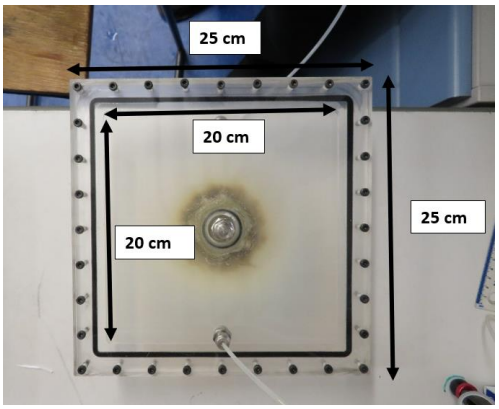

Figure 5. Dimensions of the 3-mm fracture aperture experimental setup.

Figure 5 shows the top view and dimensions of the 3-mm aperture experimental setup. Following essential things and devices needed to perform the experiments are prepared, the investigation is formed equipped to begin, as displayed in Figure 6.

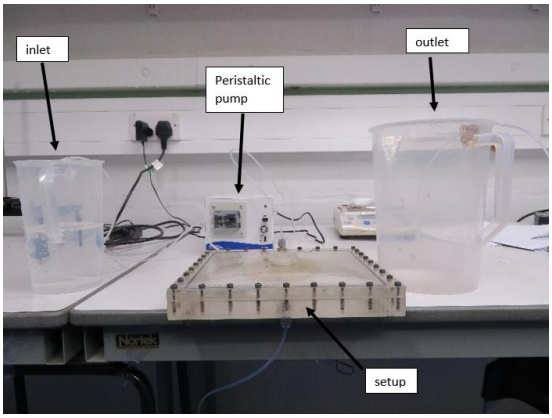

Figure 6. General view of experimental setup.

Figure 6 shows the peristaltic pump, inlet, outlet and perspex containing bentonite.Owing to higher erosion when interacting with distilled water,water with reduced strenght was utilized during investigation.

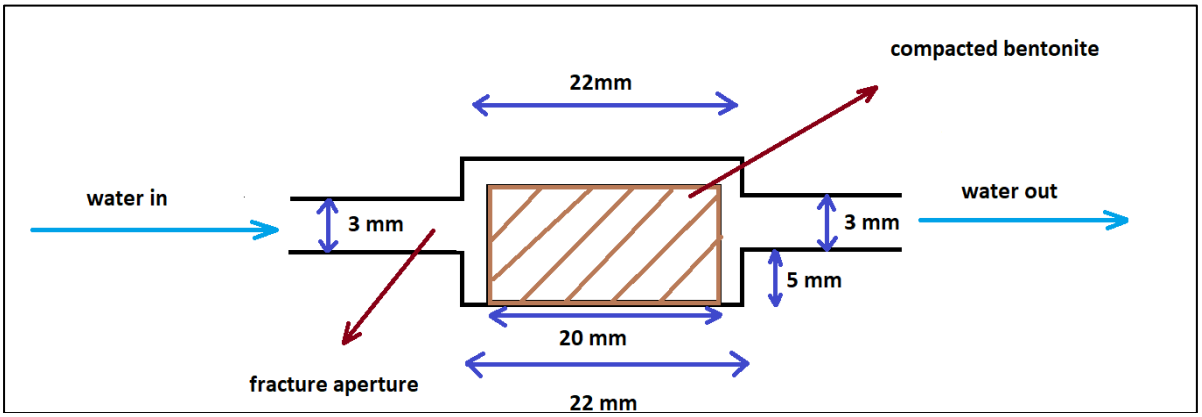

Figure 7. Cross-section of the test setup with 3-mm aperture.

Figure 7 shows the cross-section and dimensions of the experimental setup containing the bentonite used in the experiment.

2.4 Calculation of mass of eroded compacted bentonite

Dynamic light scattering (DLS) is a method in fundamental science that can be used to discover the dimension dispersal figure of tiny pieces in a heterogeneous mixture in which the solid particles are spread throughout the liquid without dissolving in it. Classic implementations of this method are the definations of tiny pieces in terms of particle size in liquid. The Brownian movement of tiny pieces or molecules in liquid-solid mixture leads laser light to disperse at dissimilar strengthes. Examination of these solidity variations grants the acceleration of Brownian movement and hence the tiny piece dimension (Berne and Pecora, 2000).

DTS0012 disposable plastic cells were used for measurement in the Malvern Panalytical Zetasizerultra instrument. These plastic cells were filled with a certain volume of samples stored in plastic tubes and made ready for measurements.

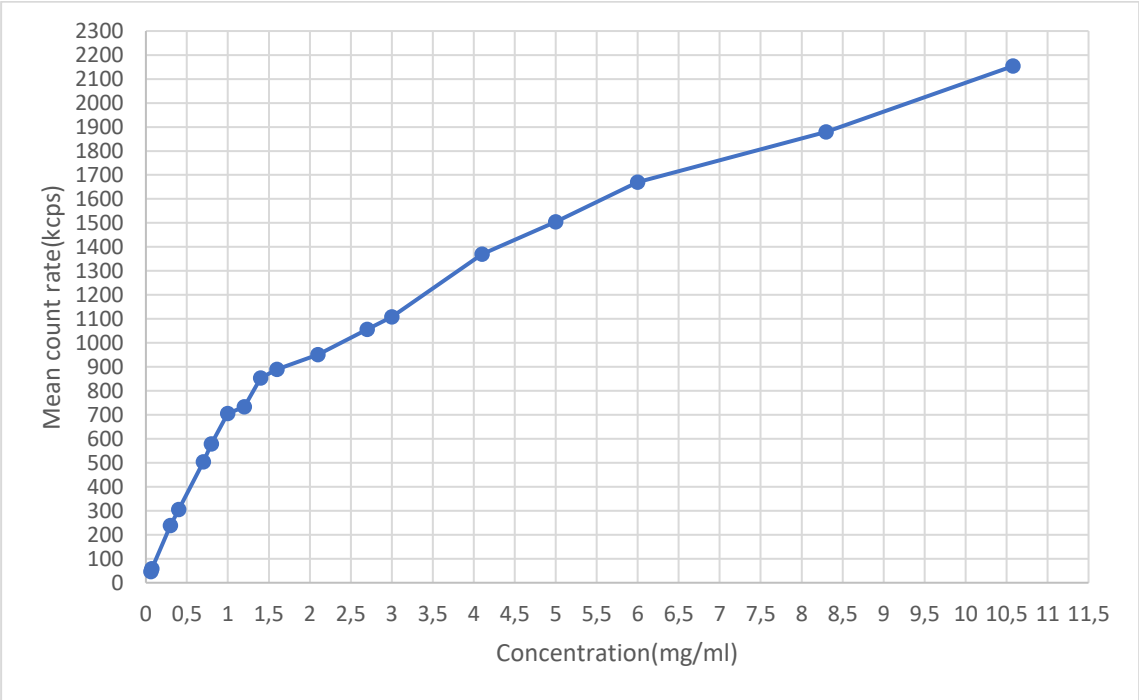

Figure 8. Calibration curve for dynamic light scattering measurements.

The relationship between mean count rate and concentration is presented in Figure 6. The mean count rate value obtained in dynamic light scattering measurements is utilized in the adjustment curve. The accumulation worth corresponding to each mean count value is obtained as seen in figure 8. The amount of eroded material is obtained by multiplying this worth with the mass of the liquid found. Throughout the investigation, images were gotten to examine the enlargement of the clay on the 8th, 16th and 24th days as seen in figure 9.

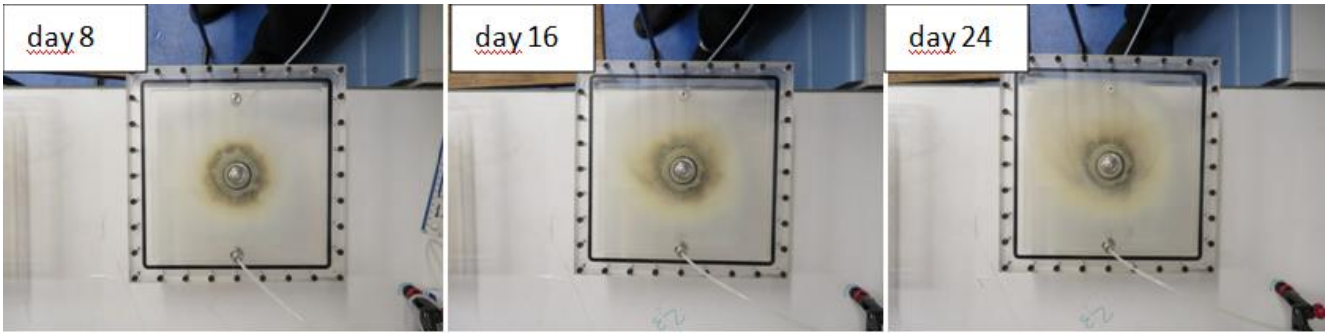

Figure 9. View of swelling compacted bentonite. (5.74 grams, 1.67g/cm3, 0.061ml/min).

AutoCAD programme was employed to measure the enlargement area. The dimensions of the 3 mm fracture aperture test rig are 25 cm * 25 cm as presented in figure 5. This results in a covered area of 625 square centimetres for the testing device in Figure 10 (a).

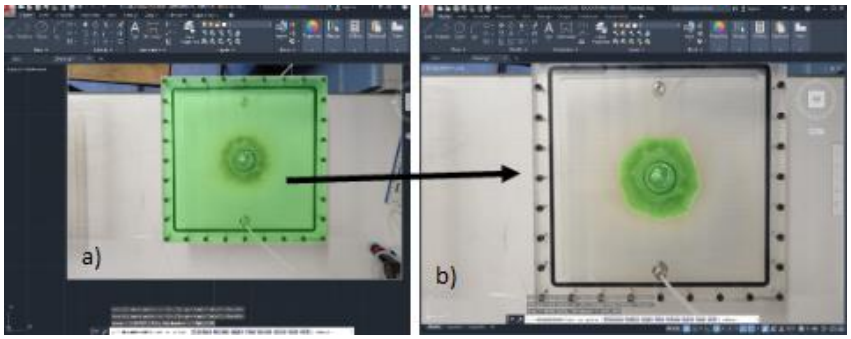

Figure 10: (a) Total area of experiment setup (b) Scanned areas of enlargement of compacted bentonite.

If this photo is installed in AutoCAD and scanned, the programme shows us the scanned area in units. After that, only the part covered by the swelling bentonite is scanned (in figure 10 b), not the entire test setup, and this scanned part is measured by the AutoCAD programme and presented as a unit. Because we have scanned the entire first experimental setup and know the actual area of this scanned part, we calculate the area of the swelling bentonite using the ratio.

3. Results and discussion

It is observed that the amount of eroded material increases with increasing the flow rate. Figure 11 shows the total amount of erosion that occurred during the experiment. The flow rates applied throughout the experiment were 0.09 ml/min, 0.127 ml/min, 0.168 ml/min and 0.22 ml/min. The amounts of erosion corresponding to these flow rates are 1883.9742 mg, 1809.5545 mg, 2197.9064 mg and 2180.78 mg respectively.

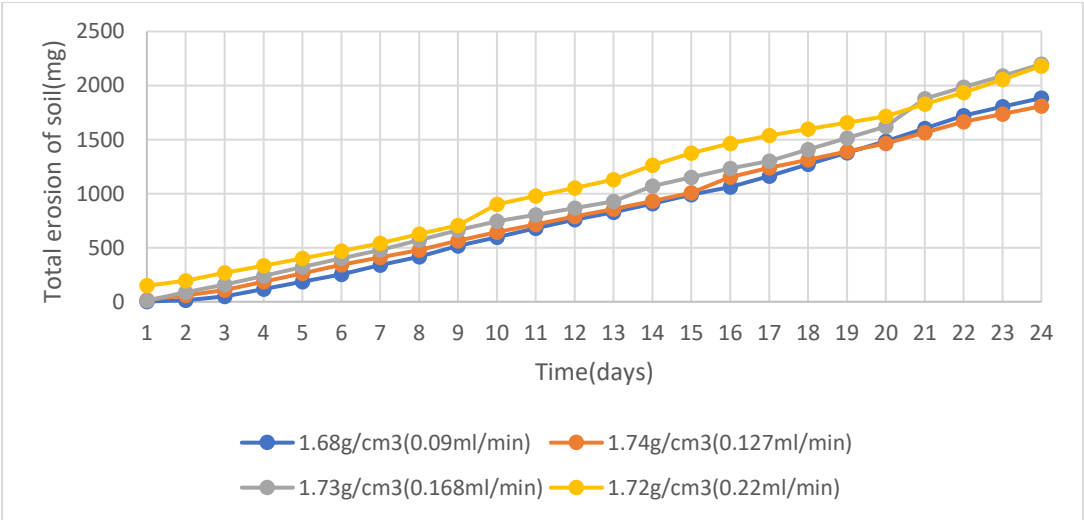

Figure 11. Amount of eroded compacted bentonite.

The total erosion amounts at the end of each day according to the flow rates are shown in Table 3.

Table 3. Total erosion amounts at the end of each day according to flow rates.

Days	Total erosion(mg)			
	1,68 g/cm3 0,09ml/min	1,74 g/cm3 0,127 ml/min	1,73 g/cm3 0,168 ml/min	1.72 g/cm3 0.22 ml/min
1	2,17	17,80	10,88	148,50
2	14,09	58,24	86,60	195,30
3	50,35	107,90	157,53	267,80
4	118,16	185,64	239,21	334,50
5	185,97	263,37	320,88	401,20
6	253,78	341,11	402,56	467,90
7	337,78	410,20	478,92	539,90
8	415,43	477,83	570,96	626,30
9	516,75	564,79	662,27	707,30
10	597,89	642,79	743,30	902,30
11	679,02	715,76	805,15	977,90
12	760,16	788,74	867,00	1053,50
13	827,02	857,47	928,85	1129,10
14	908,37	930,77	1070,81	1263,30
15	991,46	1008,04	1148,98	1376,22
16	1061,91	1153,41	1233,66	1463,37
17	1162,64	1237,81	1300,30	1536,61
18	1270,41	1313,37	1407,13	1596,00
19	1378,19	1388,93	1513,96	1655,39
20	1485,97	1464,49	1620,79	1714,78
21	1604,30	1564,16	1877,44	1826,78
22	1722,64	1663,84	1984,95	1934,78
23	1803,31	1736,70	2088,33	2054,78
24	1883,97	1809,55	2197,91	2180,78

Investigations should be performed at low hydraulic conditions, till 5% of the beginning dried is abraded. In conformity with buffer collapse standard of Svensk Kärnbränslehantering Aktiebolag (SKB), compacted bentonite cannot be eroded by more than five percent (Reid, 2015). Based on this information, the percentages of the erosion amounts obtained during the 24-day experiment to the dry amounts of the compacted bentonite samples were calculated. The specimen with a dry density of 1.68 g/cm^3 and exposed to a flow rate of 0.09 ml/min eroded 35.19% of its initial mass at the last of the investigation. The specimen with a dry density of 1.74 g/cm^3 and exposed to a flow rate of 0.127 ml/min eroded 32.71% of its initial mass at the last of the investigation. The specimen with a dry density of 1.73 g/cm^3 and exposed to a flow rate of 0.168 ml/min eroded 40.46% of its initial mass at the end of the experiment. Finally, the sample with a dry density of 1.72 g/cm^3 and exposed to a flow rate of 0.22 ml/min eroded 40.29% of its initial mass at the end of the experiment. As can be seen from the experiment results, the erosion percentages obtained are above the 5 percent rate determined by the SKB.

Taking into account the five percent erosion standard, the time that treated compressed bentonite eroded by 5 percent from the lowest flow rate to the highest flow rate, respectively, are the 17th and 18th days for 0.02 ml/min, the 7th and 8th days for 0.061 ml/min, day is 9th and 10th days for 0.09ml/min, 7th and 8th days for 0.127ml/min, 5th and 6th days for 0.168ml/min and 4th and 5th days for 0.22ml/min.

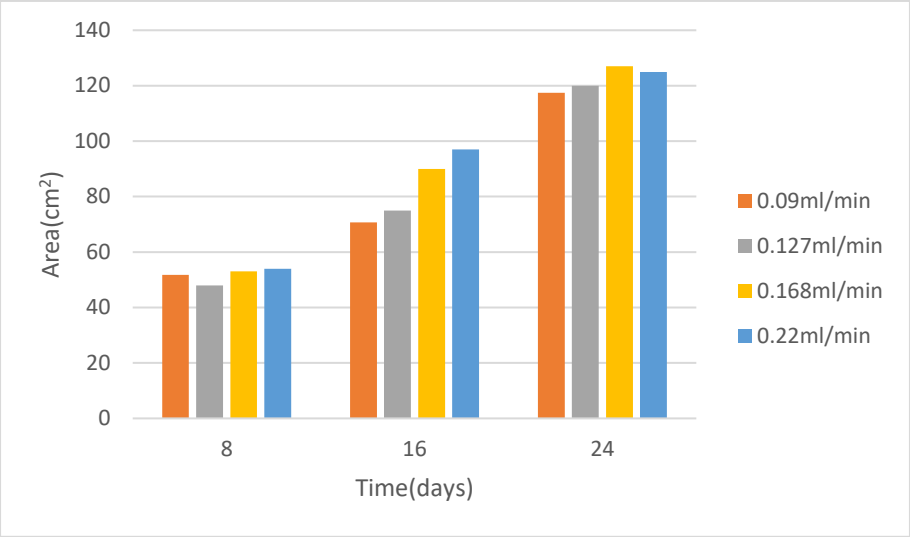

Figure 12. Expansion amounts depending on flow rates.

Figure 12 illustrates the swelling area of compacted bentonite into a 3 mm fracture. The area swollen in the first eight days is 51.76 cm^2 and 70.7 and 117.5 cm^2 on days 16 and 24, respectively for 0.09 ml/min. The area swollen in the first eight days is 48 cm^2 and 75 and 120 cm^2 on days 16 and 24, respectively for 0.127 ml/min. The area swollen in the first eight days is 53 cm^2 and 90 and 127 cm^2 on days 16 and 24, respectively for 0.168 ml/min. The area swollen in the first eight days is 54 cm^2 and 97 and 125 cm^2 on days 16 and 24, respectively for 0.22 ml/min. The expansion of the compressed bentonite constantly grew with the rise of the flow rate, relying on the flow rate.

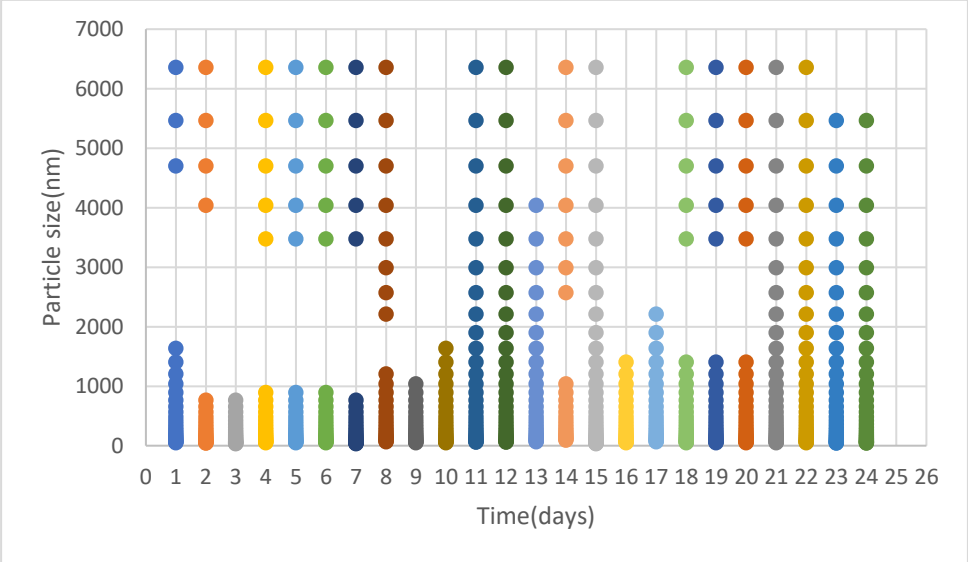

Figure 13. Daily observed particle sizes (5.83 grams 1.68 g/cm^3 (0.09 ml/min)).

Figure 13 shows the size dispersal of the eroded particles of compressed bentonite under a flow rate of 0.09 ml/min. The largest particle size is 6358 nanometers, and the smallest particle size is 50.79 nanometres. Except for the 3rd, 9th, 10th, 16th and 17th days, the sizes of the eroded particles are between these two values.

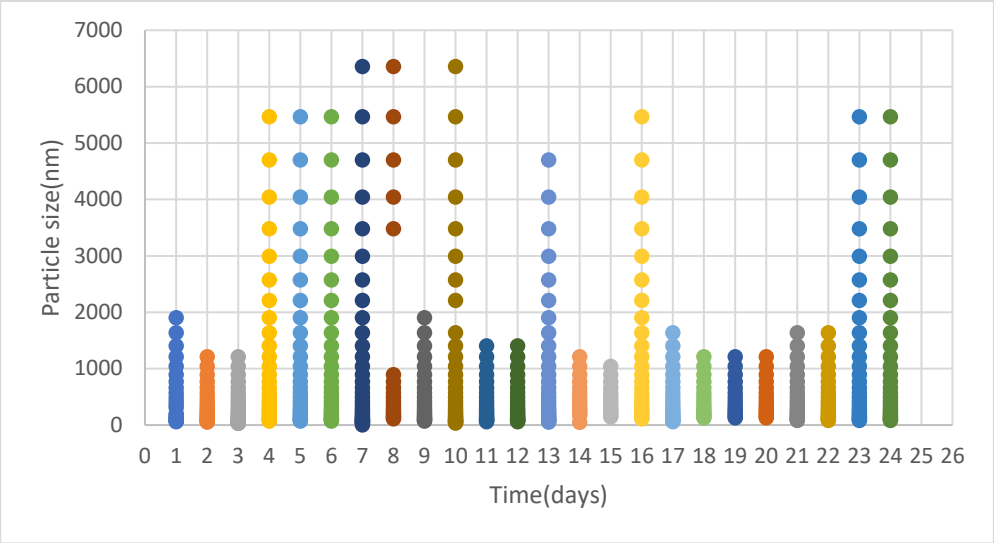

Figure 14. Daily observed particle sizes (6.02 grams 1.74 g/cm^3 (0.127 ml/min)).

Figure 14 displays the size distribution of the eroded particles of compacted bentonite under a flow rate of 0.127 ml/min. The largest particle size is 6358 nanometers, and the smallest particle size is 50.79 nanometres. For 14 days of the 24-day experimental period, particle sizes were between 50.79 nanometres and 2000 nanometres.

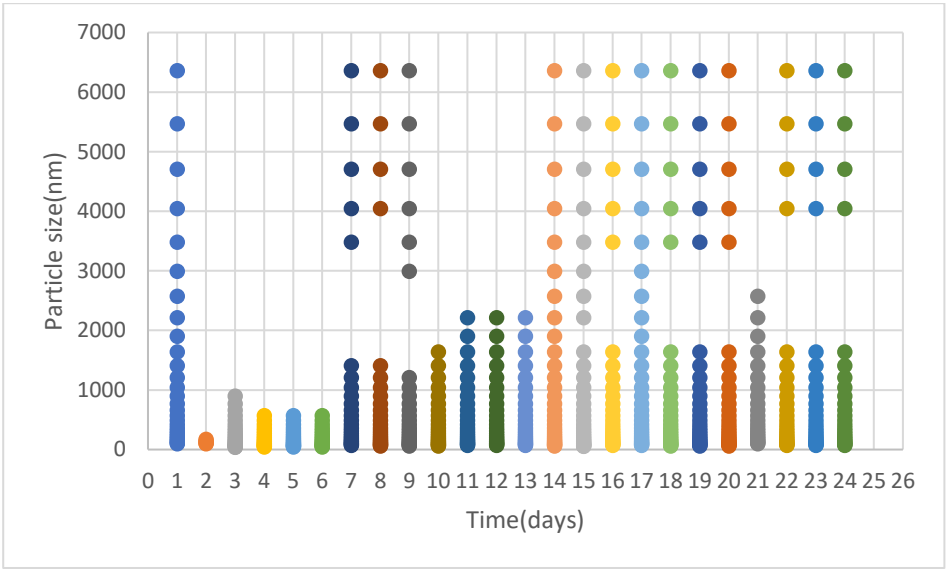

Figure 15. Daily observed particle sizes (5.92 grams 1.73 g/cm^3 (0.168 ml/min)).

Figure 15 displays the size dispersal of the eroded particles of compressed bentonite under a flow rate of 0.168 ml/min. The largest particle size is 6358 nanometers, and the smallest particle size is 50.79 nanometres. On the 2nd, 3rd, 4th, 5th and 6th days, particle sizes ranged between 50.79 nanometres and 1000 nanometres, while the other days ranged between 50.79 nanometres and 6358 nanometres.

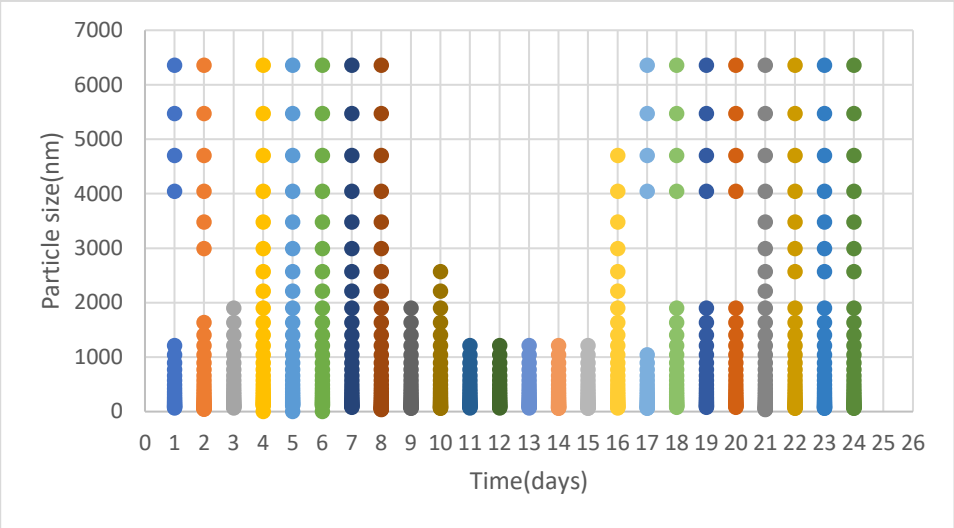

Figure 16. Daily observed particle sizes (5.89 grams 1.72 g/cm^3 (0.22 ml/min)).

The size distribution of compacted bentonite particles eroded under 0.22 ml/min flow rate is shown in Figure 16. Except between 9th and 15th days, the eroded bentonite particle sizes were observed between 50.79 nm and 6358 nm. Throughout the experiment, the sizes of the eroded bentonite particles were obtained through the Malvern panalytical zetasizer. No relationship between flow rate and eroded bentonite particles could be detected.

SKB's present quantitative safety status model is based on a buffer consisting of 100% purified sodium montmorillonite. SKB's model measures the montmorillonite release rate from a conductive fracture that cuts a 1.75 m diameter sedimentation hole according to equation 1.

$$R_{Erosion} = A \times \delta \times v^{0.41} \quad (1)$$

Where: $R_{Erosion}$ = release rate (kg/year), A = constant 27.2, δ = fracture aperture (m) and v = groundwater velocity (metres/year).

A dynamic force balance model is used to predict radial extrusion of the buffer to fracture for various groundwater chemistries. This considers all the forces acting on each montmorillonite particle, which are gravitational and buoyant forces, diffusion, Van der Waals gravity, diffuse bilayer thrust and frictional forces (Moreno et al. 2010). Advective erosion of the buffer from the buffer-groundwater interface is modelled by simultaneous solving of the Darcy flow equation (for two-dimensional flow in a fracture), the solute diffusion equation, and the dynamic force balance equations for expansion of the gel for dilute groundwater chemistries. Equation 1 is originated from this method, which calculates a constant rate of mass loss from the buffer-groundwater interface at the fracture when a steady state between extrusion and erosion is reached for a given groundwater chemistry, velocity, and fracture opening.

Table 4. Comparison experiment results with calculation based on equation 1.

Experiments (according to flow rates)	Calculation	Experiment results (dynamic light scattering)
0.09 ml/min	5725 mg	1883 mg
0.127 ml/min	6474 mg	1809.55 mg
0.168 ml/min	7310 mg	2197.9 mg
0.22 ml/min	8270 mg	2180.78 mg

We should remember that the equation used is presented based on the 1.75-meter diameter system. In their simulations, Moreno et al. (2010) looked at how the sedimentation hole diameter affects the montmorillonite release rate by both increasing the deposition hole to 5 m and reducing the deposition hole to 0.5 m. The results of these simulations are shown in figure 17.

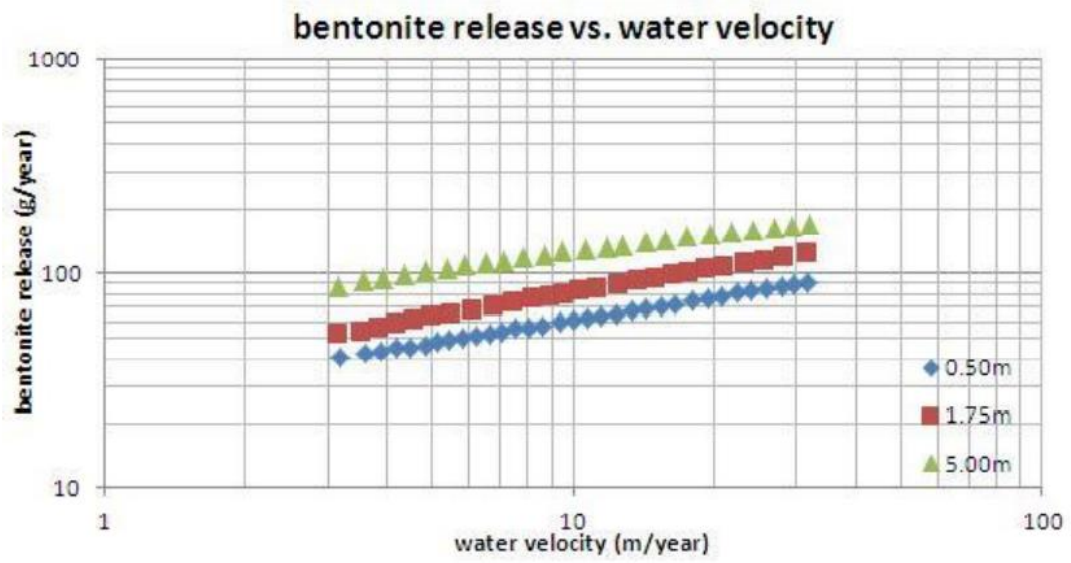

Figure 17. Montmorillonite mass loss against water velocity for various deposition hole diameters. 1mm fracture aperture. Adapted from Moreno et al (2010).

As seen in figure 17, the water velocity values are above the values we used in our experiments. While obtaining the flow velocity values from the flow rate values, we considered the area where the flow rate is effective as the water area inside the system. This value is 400 cm^2. The lowest values in Figure 17 were used to evaluate the erosion rate in our 0.02 m diameter system.

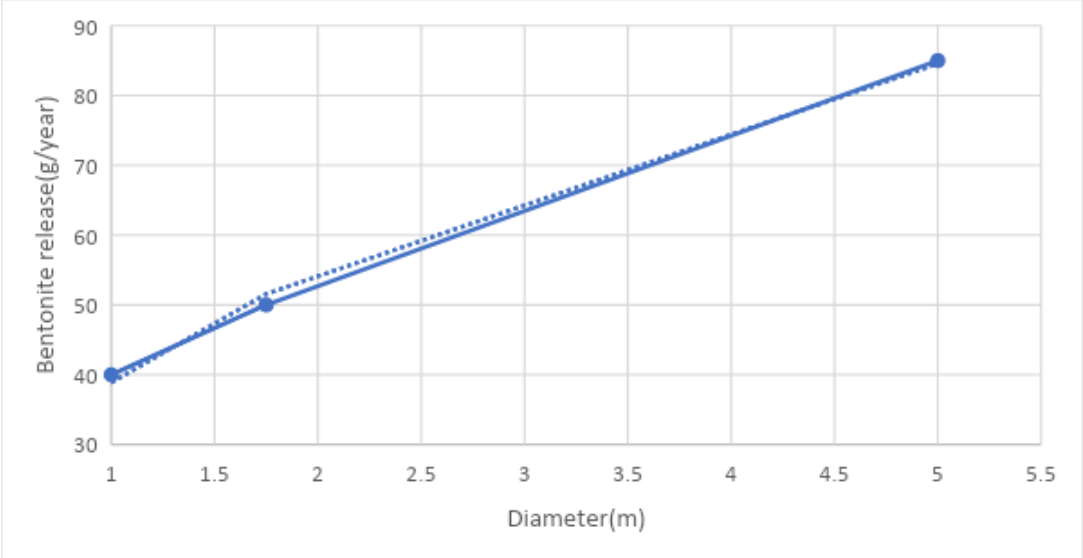

Figure 18. Bentonite release rate and diameter relationship.

Figure 18 shows the relationship between bentonite release and the diameter of the compacted bentonite. Using the equation 1 in Figure 18, the bentonite release value that will occur in our 0.02 diameter system is obtained as 34 m/year. The bentonite release value in the 1.75 m diameter system is 50 m/year. When these values are compared to each other, it is understood that the values in equation 1 should be multiplied by the coefficient of 0.68. Thus, the values in Table 5 are obtained.

Table 5. Converted values and experiment results comparisons.

Experiments (according to flow rates)	Calculation	Experiment results (dynamic light scattering)
0.09 ml/min	3893 mg	1883 mg
0.127 ml/min	4402 mg	1809.55 mg
0.168 ml/min	4970 mg	2197.9 mg
0.22 ml/min	5623 mg	2180.78 mg

Since the calculation in equation 1 is based on 100% purified sodium montmorillonite and the erosion rate in the equation is constant regardless of time, it makes sense that the calculated erosion is higher than the actual erosion values. We know from experiments that the rate of erosion is not constant.

In the Miller and Vilks work (2010), flow rate up to 900 millilitres is 0.1 ml/min. This corresponds to approximately 150 hours, or 6.25 days. As we can see from the figures (from Miller and Vilks), the bentonite concentration is 150 mg/L up to 900 millilitres. When we convert this value to 900 millilitres, we get 135 mg. This value represents the total erosion. If we accept that the erosion is linear for the first 7 days, this value corresponds to 151.2 milligrams. The weight of bentonite used was 21.5 grams, the ratio of montmorillonite was 80% and the dry density was 2 g/cm3. The fracture aperture in the experimental setup is 5 mm. The bentonite we used has a weight of 5.83 grams, a dry density of 1.68 g/cm3 and a montmorillonite ratio of 96.8%. Also, the fracture aperture in our experimental setup is 3 mm. In Figure 19, despite all these differences, some assumptions were made to compare the results of two experiments with close flow rates. The results with 3 mm aperture are taken from our experimental results subjected to a flow rate of 0.09 ml/min.

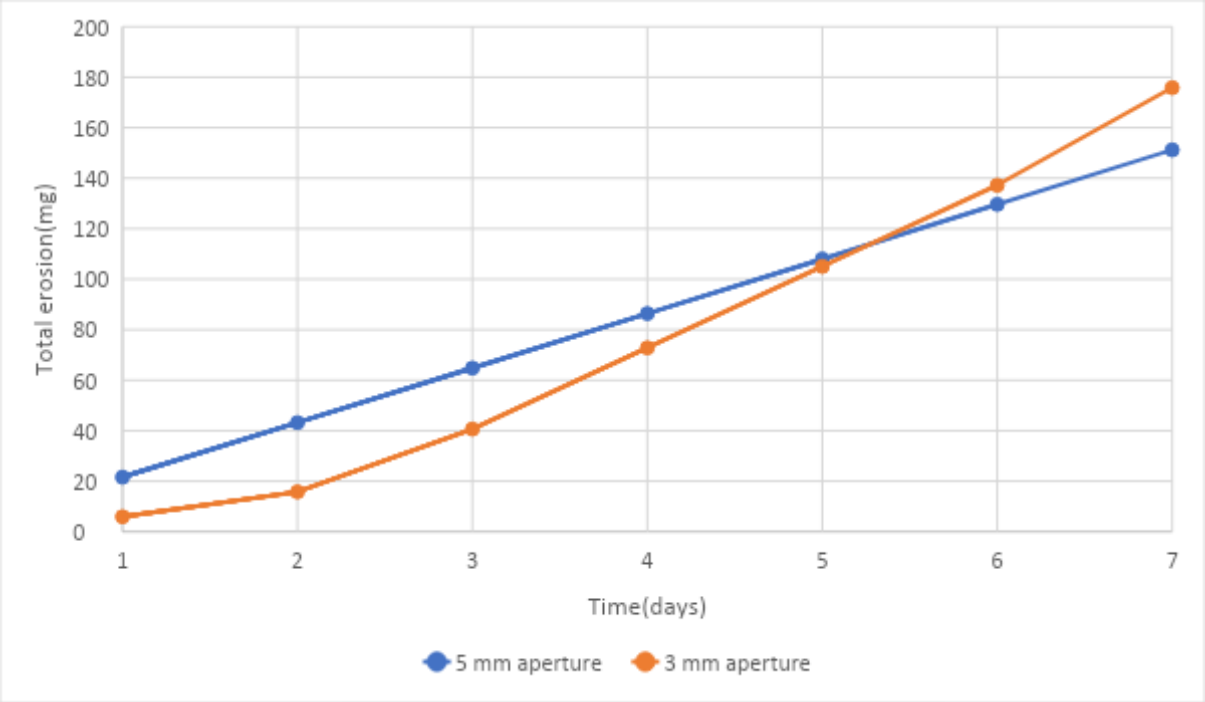

Figure 19. Erosion comparison between 3mm and 5mm set-ups (in 5mm set-up, erosion is accepted as linear).

Comparison of the results of these two experiments will not give reliable results due to the differences in bentonite weights, bentonite dry density values, fracture openings, flow rates and smectite ratios contained in bentonites. Despite this, it is tried to be shown in figure 19.

In the study of Timothy Schatz (2013), the results obtained are not comparable to the results of our experiments due to the difference in the dry density of bentonite, the proportions of montmorillonite contained in bentonite, the applied flow rates, the fracture opening of the experimental setup and the weight of the compacted bentonite.

4. Conclusion

In order to investigate the possible erosion of water inlet during the storage of spent nuclear waste material in underground repositories, water inlets with flow rates of 0.09 ml/min, 0.127 ml/min, 0.168 ml/min and 0.22 ml/min were simulated. The amounts of erosion corresponding to these flow rates, the size of the bentonite particles eroded daily, and the expansion of the compacted bentonite are presented. What is unclear here is what size of bentonite particles transport radionuclides when radionuclides are transported by bentonite. Since this question has not been answered so far, the influence of different hydraulics on the size of eroded bentonite particles will be important in the future when the relationship between radionuclide sorption and the size of eroded bentonite particles is found. There is no other study in the literature that simultaneously presents the amount of erosion of compacted bentonite, the size of the eroded particles and the expansion of the compacted bentonite during this period under water flow rate. The findings of the study show that with increasing flow rate, the expansion of compacted bentonite increases, and the amount of eroded bentonite particles increases. Although no correlation was found between the sizes of eroded particles corresponding to the applied flow rates, the daily presentation of the sizes of eroded particles at these flow rates will be important in the future when the relationship between the size of the radionuclide and the size of the bentonite particles that absorb it is found.

Suggestions for future experiments are as follows:

- The investigations were conducted at room temperature. The experiments should be repeated at other temperature values by keeping the experimental variables constant. Thus, the effect of temperature on erosion can be observed.
- The effect of ions on erosion can be observed by using water with ionic value instead of distilled water.
- Instead of 3 mm fracture aperture, fracture aperture values can be changed, and erosion values can be obtained at different fracture aperture values and the effect of fracture aperture (contact surface) on erosion can be analysed.
- The effect of montmorillonite content on erosion can be measured by repeating the experiments with bentonites having different values of montmorillonite content.

Acknowledgements
I would like to thank Dr Majid Sedighi for his help throughout this study.

References

AB, S. K. (2011). Long-term safety for the final repository for spent nuclear fuel at Forsmark.
Vilks, P., & Miller, N. H. (2010). Laboratory bentonite erosion experiments in a synthetic and a natural fracture. *Nuclear Waste Management Organization Report NWMO TR-2010-16. Toronto, Ontario*.

Baik, M. H., Cho, W. J., & Hahn, P. S. (2007). Erosion of bentonite particles at the interface of a compacted bentonite and a fractured granite. *Engineering Geology*, *91*(2-4), 229-239.

Berne, B. J., & Pecora, R. (2000). *Dynamic light scattering: with applications to chemistry, biology, and physics*. Courier Corporation.

Bülbül,S. (2022). "The effect of flow rate on the erosion of physically purified compacted bentonite", MACE PGR Conference Proceeding Book, 56-60, Manchester University, 01 July 2022.

Chapman, N. A., & Mc Kinley, I. G. (1987). The geological disposal of nuclear waste.

Cho, W. J., Lee, J. O., Chun, K. S., & Park, H. S. (1999). Analysis of functional criteria for buffer material in a high-level radioactive waste repository. *Nuclear Engineering and Technology*, *31*(1), 116-132.

Coons, W. E., Moore, E. L., Smith, M. J., & Kaser, J. D. (1980). *Functions of an engineered barrier system for a nuclear waste repository in basalt* (No. RHO-BWI-LD-23). Atomics International Div., Richland, WA (USA). Rockwell Hanford Operations.

Geckeis, H., Schäfer, T., Hauser, W., Rabung, T., Missana, T., Degueldre, C., ... & Alexander, W. R. (2004). Results of the colloid and radionuclide retention experiment (CRR) at the Grimsel Test Site (GTS), Switzerland–impact of reaction kinetics and speciation on radionuclide migration.

Gong, Z., Liao, L., Lv, G., & Wang, X. (2016). A simple method for physical purification of bentonite. *Applied Clay Science*, *119*, 294-300.

Grindrod, P., Peletier, M., & Takase, H. (1999). Mechanical interaction between swelling compacted clay and fractured rock, and the leaching of clay colloids. *Engineering Geology*, *54*(1-2), 159-165.

Kurosawa, S., Kato, H., Ueta, S., Yokoyama, K., & Fujihara, H. (1999). Erosion properties and dispersion-flocculation behavior of bentonite particles. *MRS Online Proceedings Library (OPL)*, *556*, 679.

Missana, T., Alonso, Ú., & Turrero, M. J. (2003). Generation and stability of bentonite colloids at the bentonite/granite interface of a deep geological radioactive waste repository. *Journal of Contaminant Hydrology*, *61*(1-4), 17-31.

Moreno, L., Neretnieks, I., & Liu, L. (2010). Modelling of erosion of bentonite gel by gel/sol flow

Reid, C., Lunn, R., El Mountassir, G., & Tarantino, A. (2015). A mechanism for bentonite buffer erosion in a fracture with a naturally varying aperture. *Mineralogical Magazine*, *79*(6), 1485-1494.

Schäfer, T., Huber, F., Seher, H., Missana, T., Alonso, U., Kumke, M., ... & Enzmann, F. (2012). Nanoparticles and their influence on radionuclide mobility in deep geological formations. *Applied geochemistry*, *27*(2), 390-403.

Schatz, T., Kanerva, N., Martikainen, J., Sane, P., Olin, M., Seppälä, A., & Koskinen, K. (2013). *Buffer erosion in dilute groundwater* (No. POSIVA--12-44). Posiva Oy.